Penetration mechanisms of surface-adsorbed hydrogen atoms into bulk metals: Experiment and model

Markus Wilde* and Katsuyuki Fukutani
Institute of Industrial Science, University of Tokyo, 4-6-1 Komaba, Meguro-ku, 153-8505 Tokyo, Japan
and CREST-JST, 4-6-1 Komaba, Meguro-ku, 153-8505 Tokyo, Japan
(Received 5 February 2008; revised manuscript received 6 August 2008; published 9 September 2008)

The conditions enabling the transition of surface-adsorbed hydrogen atoms into bulk metals are explored by comparing the response of chemisorbed H on Pd(100) and Ti(0001) single crystals to thermal activation in vacuum. Thermal desorption spectroscopy and $^{1}H(^{15}N,\alpha\gamma)^{12}C$ nuclear reaction analysis reveal that heating causes H_2 desorption from Pd(100), whereas H atoms on Ti(0001) reversibly exchange between the surface and the Ti bulk with negligible desorption loss of H_2. A general model is proposed in which the competition between desorption and bulk absorption of surface hydrogen is, on one hand, kinetically determined by the activation energy for associative H_2 desorption relative to the effective energy barrier for H absorption. On the other hand, the thermodynamic possibility to dissolve the surface H atoms into the metal must be considered to consistently explain the opposite behavior of H on Pd(100) and Ti(0001). The first experimental estimation of the energy of surface adsorption, $\varepsilon_s=-0.92$ eV, for H/Ti(0001) is presented, in good agreement with theoretical calculations.

DOI: 10.1103/PhysRevB.78.115411 PACS number(s): 82.65.+r, 82.20.Kh, 68.43.−h, 68.47.De

I. INTRODUCTION

The bidirectional transport of hydrogen atoms across metal surfaces is fundamentally important for the reversible formation and decomposition of metal hydrides, which find numerous applications as hydrogen permeation purifiers, "switchable" mirrors, storage alloys, and getter pumps. Palladium and titanium are frequently used materials in such devices, since both dissociate H_2 molecules on their surfaces without appreciable activation barriers and absorb hydrogen exothermically into their bulk. Although H adsorption on Pd (Refs. 1–5) and Ti (Refs. 6–11) surfaces and its bulk solution[12–15] have been characterized in appreciable detail, certain open questions concerning the exact penetration mechanism of their surfaces by hydrogen still remain. Since in metal-H systems the energy of surface adsorption is generally much higher than the heat of bulk solution,[16] the exposure of a H-free metal to H_2 gas will at first cause rapid and preferential filling of the surface adsorption sites, before hydrogen is absorbed into the bulk on a much longer time scale, because the difference between the surface adsorption and bulk solution enthalpies comprises an inevitable activation barrier along the absorption path into the bulk. Thus, at moderate temperatures and H_2 pressures (where H is stable on the surface) gaseous H_2 molecules interact with a metal surface which is occupied with dissociated H atoms near saturation coverage. In this situation the ambiguity arises as to whether the preadsorbed H atoms equilibrated at majority adsorption sites penetrate into the bulk, or if the absorbed H stems mainly from H_2 molecules that dissociate and enter into the metal lattice on alternative pathways, for instance at certain defect sites that may offer preferential penetration channels of lower activation barriers than the regular terrace sites. In the reverse process, the release of hydrogen from the metal bulk into the gas phase, the analog problem concerns the exact location in the surface where the H atoms resurface from the bulk before they recombine and desorb as H_2 molecules, and whether the recombination involves the surface-adsorbed H atoms. Hence, the central question is whether the reaction coordinate for the transition of hydrogen between the gas phase and the metal bulk includes the energy minimum of the surface chemisorption potential well at *regular* terrace sites.

This paper thus explores the conditions under which H absorption becomes a *majority* effect: We clarify the factors that determine whether or not surface-adsorbed H atoms accommodated in the potential minima of regular chemisorption sites participate in the surface penetration. This specific detail of the H absorption mechanism has scarcely found attention so far,[14] particularly not in the case of the much less extensively studied titanium. As our focus is the fate of chemisorbed H atoms, we elucidate this problem with a unique experimental approach that excludes gaseous H_2. We discriminate chemisorbed surface H from absorbed H beneath the surface by depth-resolving and H-specific $^{1}H(^{15}N,\alpha\gamma)^{12}C$ nuclear reaction analysis (NRA). By cross-referencing their respective temperature-dependent NRA signatures with thermal desorption spectroscopy (TDS) it can then be clearly distinguished, whether the surface H atoms either desorb into the vacuum or penetrate into the bulk upon thermal activation. The comparison of H on Pd(100) and Ti(0001) surfaces will show that each represents exactly one of these opposite extremes. A general scheme is developed that enables us to predict the outcome of the desorption-versus-bulk-absorption competition, which in the simplest case is determined only by the enthalpies of H surface adsorption, bulk solution, and the activation energy of H diffusion in the bulk. In particular we point out that two criteria need to be fulfilled simultaneously for H absorption to occur: Both the kinetic-energy barriers of the competing absorption/desorption reactions and the thermodynamic condition, whether the metal bulk offers sufficient solubility to absorb the layer of surface H atoms, must favor H absorption.

II. EXPERIMENT

A single crystal of Pd(100) ($10\times7\times1.5$ mm^3) or Ti(0001) ($5\times5\times1.5$ mm^3) was suspended on an ultrahigh vacuum (UHV) sample holder attached to a liquid nitrogen reservoir by spot welding to tantalum support rods, enabling to cool the sample to a minimum temperature of ~100 K. Heating was performed with a *W* filament behind the sample by either thermal radiation or electron bombardment. A chromel-alumel thermocouple spot-welded to the crystal side was used for temperature monitoring. H_2-TDS measurements were performed at a heating rate of 1 K/s with a shielded and differentially pumped quadrupole mass spectrometer (Balzers QMS Prisma). Ar-ion sputtering and annealing cycles were used to clean the surfaces from contaminants and to establish long-range atomic order as confirmed by Auger electron spectroscopy (AES) and low-energy electron diffraction (LEED). Additional O_2 annealing/flashing cycles were carried out to remove residual carbon impurities from Pd(100), until the H_2 thermal desorption spectrum after exposure to 5 L H_2 at 100 K reproduced the published desorption temperature of chemisorbed H from the clean surface.[2,14] Temperatures in excess of 970 K and prolonged annealing were avoided in case of the hcp α-Ti(0001) crystal in order to exclude the occurrence of the phase transition to the cubic bcc Ti β-phase at 1155 K (Ref. 12) and to prevent segregation of sulfur and chlorine impurities from the Ti bulk. Both samples exhibited clear LEED patterns with bright and sharp diffraction spots on a low background after the respective cleaning procedures. Still, small amounts of O and C (max 5%) remained even after our best cleaning efforts on the particularly reactive Ti(0001) surface. These residual impurities, however, were judged to be insignificant because the freshly cleaned Ti(0001) surface yielded near-surface NRA H depth profiles of excellent reproducibility after hydrogen exposure at 100 K, which otherwise turned out to be quite sensitive to the presence of impurities, in particular oxygen, which blocks the H uptake. Residual H_2O adsorption was noticed only after extended experiments (~90 min) on a cooled sample, but not in this study. Hydrogen exposures are given in Langmuir (1 L=1 $\times10^{-6}$ Torr s), where the H_2 pressures were taken directly from the Bayard/Alpert ionization gauge readings without further sensitivity correction. A mixture of atomic H and molecular H_2 was dosed in some experiments via a molybdenum tube directed at the sample from ~100 mm distance, which contained a *W* filament heated at 1700 K to partially dissociate the H_2 gas. The UHV system used for the sample preparation and NRA/TDS measurements has a base pressure $<1\times10^{-8}$ Pa and is attached to a dedicated beamline of the 5 MV Van de Graaff Tandem accelerator in the Microanalysis Laboratory of the University of Tokyo (MALT).

Ion beams of $^{15}N^{2+}$ at ~6.385 MeV of 20–50 nA current and 2–4 mm diameter were used to record the near-surface H depth profiles of the respective Pd(100) and Ti(0001) targets by NRA. The yield of 4.43 MeV γ-rays released in the $^1H(^{15}N,\alpha\gamma)^{12}C$ nuclear reaction between the ^{15}N ions and H in the target provides a signal proportional to the H concentration.[17,18] The ^{15}N ion energy (E_i) dependence of the γ-yield represents the convolution of the H depth distribution in the sample with the energy width of the incident ion beam ($\Delta E=3$ keV), a typically ~8–15 keV wide Gaussian Doppler broadening due to zero-point vibration of the H atoms,[19,20] energy straggling in the target,[21] and finally the narrow energy resonance ($\Gamma=1.85$ keV) of the nuclear reaction at $E_{res}=6.385$ MeV (Ref. 22). As a result of the dominating vibrational Doppler broadening, H atoms on the target surface are detected in the form of a nearly Gaussian peak at E_{res} (Ref. 23). ^{15}N ions incident at higher energies $E_i>E_{res}$ react with H below the surface after electronic stopping has decelerated them to E_{res} upon penetrating into a certain probing depth $z=(E_i-E_{res})/(dE/dz)$, where (dE/dz) is the stopping power of the material [3.90 keV/nm for Pd and 2.335 keV/nm for Ti (Ref. 24)]. At shallow depths near the surface the depth resolution is mainly limited by the width of the Doppler-broadened energy resonance peak at $E_i=E_{res}$ and typically amounts to a few nanometers at normal ion incidence on the target.

Surface H coverages on the order of a few percent of a monolayer (10^{13} cm^{-2}) and bulk H concentrations of a few 100 atomic ppm (10^{18} cm^{-3}) can routinely be detected in our system, which uses a 4-in. $Bi_4Ge_3O_{12}$ (BGO) scintillator placed 30 mm behind the sample for γ-ray detection. Quantitative measurements are possible after calibration of the γ-detection efficiency with a sample of known H concentration, in our case a thin film of H:SiN/Si(100).[25,26] Sample damage by ion-beam-generated surface defects can be neglected due to the extremely small cross section for Pd recoils with ^{15}N ions at 6.4 MeV and the low ^{15}N exposures (~1% of a monolayer ^{15}N per data point).

III. RESULTS

Beginning with Pd(100) we describe how surface-adsorbed hydrogen is discriminated from H absorbed below the surface by means of nuclear reaction analysis. Figure 1 shows the NRA γ-yield curve of hydrogen near the Pd(100) surface after exposing the cleaned sample to 300 L $H+H_2$ [$p(H_2)=1\times10^{-4}$ Pa] at 100 K. The probability of H absorption by Pd(100) from H_2 is very small [$\sim10^{-3}$ (Ref. 14)], hence atomic H was admitted in order to enforce a significant H uptake on a practical time scale on which a clean surface is maintained in UHV. At 100 K the diffusion of absorbed hydrogen into the bulk is strongly suppressed, so that a measurable H concentration builds up within a shallow region below the surface. This H-rich near-surface layer is a nonequilibrium H depth distribution and its extension into the bulk very sensitively depends on the exposure temperature.[2,14,15] The peak of the γ-yield at $E_{res}=6.385$ MeV in Fig. 1 originates from H atoms adsorbed on the Pd(100) surface. Its integral intensity corresponds to a coverage of one monolayer H atoms [1 ML=1.3 $\times10^{15}$ cm^{-2}] on Pd(100). The γ-intensity in the tail of the surface peak indicates that the atomic H exposure has caused substantial hydrogen absorption into a 5–6 nm thin layer below the surface, which contains ~0.8 ML of absorbed H.[15] From the average H concentration of 2.6% this thin layer can be assigned to the β-phase of Pd hydride ($PdH_x, x\sim0.026$).[15] These data demonstrate that the distinc-

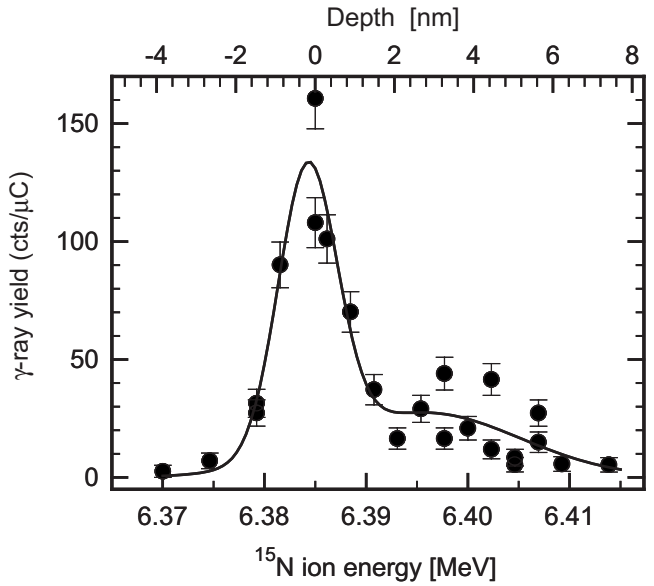

FIG. 1. NRA γ-yield curve of Pd(100) after exposure to 300 L $H+H_2$ at 100 K. Sample temperature during NRA: <150 K. The line through the experimental data points is a guide for the eye.

tion of hydrogen atoms adsorbed on the (100) surface from those absorbed in a shallow region below the surface is accomplished by means of adjusting the incident ^{15}N ion energy to collect the NRA γ-yield proportional to the H concentration at a chosen probing depth.

This technique was subsequently applied to selectively record the temperature dependences of the NRA γ-yield for hydrogen on the surface ($z=0$) and in the near-surface hydride phase at $z=6$ nm [each after a 300 L $H+H_2$ exposure of clean Pd(100) at 100 K], by measuring the remaining γ-yield after the sample temperature was increased in small increments. In Fig. 2 these data are aligned against the TDS trace, which was acquired after an identical sample preparation. It is seen that the NRA γ-signals of near-surface absorbed ($z=6$ nm) and surface hydrogen ($z=0$) sharply decrease at characteristic temperatures, i.e., 185 K and 330 K,

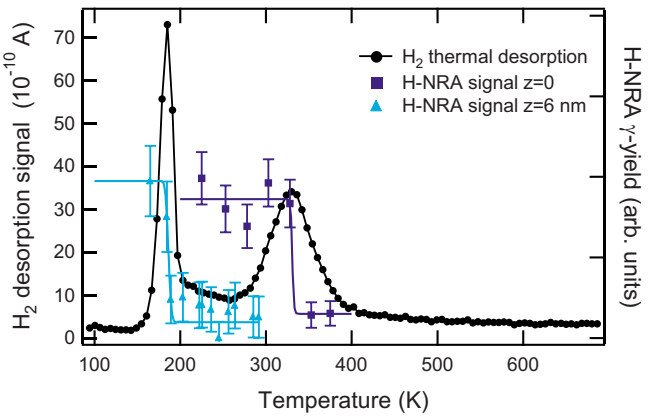

FIG. 2. (Color online) H_2 thermal-desorption spectrum of Pd(100) exposed to 300 L $H+H_2$ at 100 K and temperature dependence of NRA signals of surface ($z=0$ nm) and near-surface absorbed ($z=6$ nm) hydrogen on/in Pd(100).

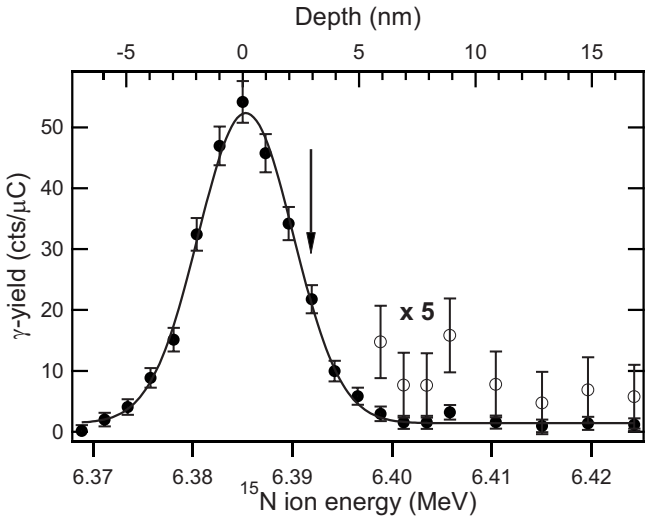

FIG. 3. NRA γ-yield curve of Ti(0001) after cleaning in UHV at $T=300$ K. The solid line is a fit of the data to the sum of a Gaussian and an error function like step profile representing H on the surface and in the bulk. The bulk H plateau is close to the detection limit but significantly above the background, as shown on the magnified ($\times 5$) scale. The arrow indicates the ^{15}N ion energy (6.3912 MeV), at which the temperature-dependent H-coverage measurements in Figs. 4 and 6 were performed.

respectively, which coincide precisely with the peak temperatures of the main desorption features in the TDS spectrum. In this way unambiguous assignments of the H_2 thermal desorption peaks are established: At 185 K absorbed hydrogen evolves by desorption during decomposition of the near-surface hydride phase whereas at 330 K the recombinative desorption of chemisorbed H atoms from the Pd(100) surface takes place. It is noteworthy for comparison to Ti(0001) and the following discussion that the thermal decay curves of the NRA signals from H on the Pd(100) surface as well as from near-surface absorbed H are accompanied by desorption of H_2, and that the near-surface absorbed H (TDS α-peak at 185 K) emerges at a lower temperature than the recombinative desorption of chemisorbed H atoms from the surface (TDS β-peak at 330 K).

In a similar fashion, hydrogen on the Ti(0001) surface is distinguished from H in the Ti bulk. The NRA γ-yield curve from the near-surface region of Ti(0001) shown in Fig. 3 exhibits a Gaussian-shaped peak at the resonance energy characteristic of surface hydrogen and a low constant plateau at 1.39 ± 0.35 cts/μC in the topmost 17 nm. Prior to this measurement the single crystal was cleaned and simply remained in UHV at 300 K during alignment of the NRA ion beam to the sample, receiving no additional H_2 exposure. Under these arbitrary conditions, the surface peak integral corresponds to a H coverage of 0.4 ML [1 ML$=1.33 \times 10^{15}$ cm^{-2} on Ti(0001)]. More importantly, the γ-yield plateau up to 17 nm indicates a bulk H concentration of (520 ± 130) at. ppm $[(2.95 \pm 0.74) \times 10^{19}$ cm$^{-3}]$, which did not measurably change during numerous surface preparations. Since any possible H concentration gradients in the single crystal level out by diffusion during the repeated high-temperature (970 K) anneals, it is reasonable to assume that

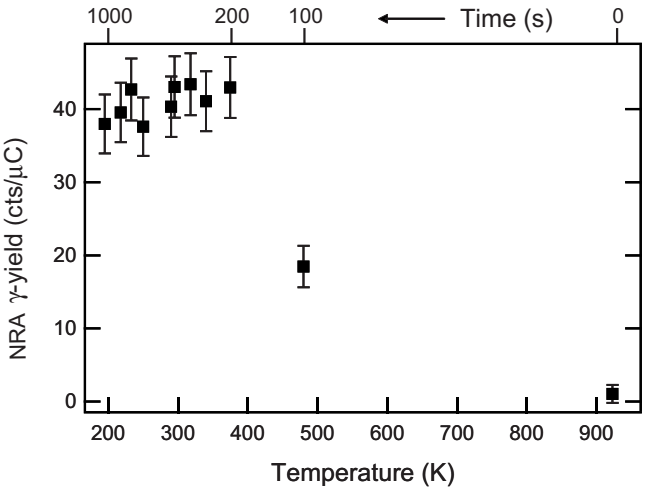

FIG. 4. Rapid evolution of the H-NRA signal on the Ti(0001) surface during cooling in UHV after flash annealing to 923 K. The acquisition time for each data point is 100 s. Upon cooling from 923 K to below 400 K within the first 200 s, the H coverage rapidly saturates at 0.5 ML (40 cts/μC at 6.3919 MeV, arrow in Fig. 3).

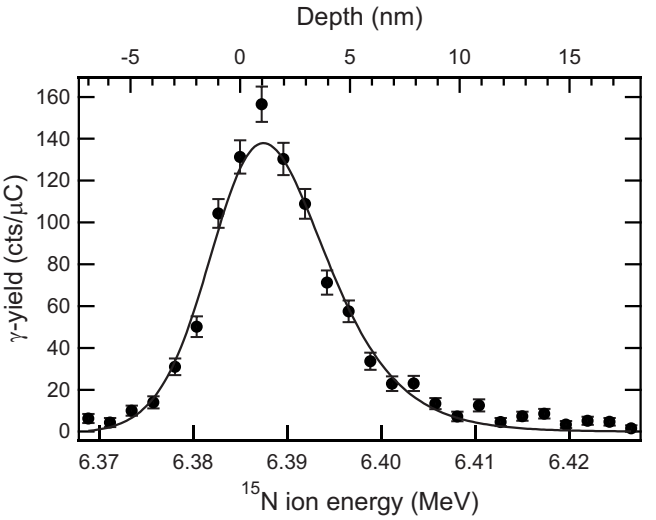

FIG. 5. NRA γ-yield curve of the H-saturated Ti(0001) single crystal (exposed to 12000 L H_2 at 120 K). The solid line is a guide for the eye.

our particular Ti(0001) specimen contained a homogeneous H impurity level of ~520 at. ppm throughout its entire thickness (1.5 mm). This non-negligible bulk H content was unexpected at first but can be rationalized by H incorporation during growth of the single crystal due to titanium's large affinity for hydrogen (heat of solution $\Delta H_s = -0.47$ eV/H atom[12]). As mentioned earlier, attempts to rid the Ti specimen from hydrogen by prolonged UHV annealing were avoided in order to prevent severe segregation of bulk impurities (S, Cl) on the surface.

The H stored in the bulk of our Ti(0001) sample gives rise to an interesting "resurfacing" effect that is evident from Fig. 4. Here, the surface H coverage was monitored continuously by NRA during a flash anneal at ~920 K and subsequent cooling of the sample to 200 K in UHV. Under these conditions the H distribution consists only of surface H and the uniformly bulk-dissolved H plateau (Fig. 3). For the temperature-dependent H coverage measurement we therefore selected a ^{15}N ion energy of 6.3912 MeV (arrow in Fig. 3), at which the γ-yield is still dominated by the Doppler-broadened surface H signal (40% of the peak maximum), yet simultaneously the bulk H concentration can be probed with improved sensitivity (84% of the plateau height in Fig. 3) compared to $E_i = E_{res}$ (50%). The small γ-signal (~1.2 cts/μC) measured near the background at 920 K in Fig. 4 is thus due to the bulk H component while the surface is completely depleted. Upon heating termination the NRA signal increased suddenly to a γ-yield of 40 cts/μC, i.e., a coverage of ~0.5 ML H emerged on the Ti(0001) surface while the Ti crystal cooled rapidly to 380 K within the first 200 s, so that only two data points could be taken. During continued slower cooling to the final temperature of 200 K, the H coverage did not increase further. The rapid initial surface H buildup (0.5 ML) is too large to be explained solely by H_2 readsorption from the UHV residual gas, although the Ti surface is known to be very reactive.[8] The H_2 exposure due to the elevated UHV background (90% H_2) right after the flash annealing ($p = 1.5 \times 10^{-8} - 1 \times 10^{-7}$ Pa) varied between 0.03–0.2 L depending on the outgassing condition of the sample holder, whereas the accumulated H coverage after cooling was always constant and reproducibly larger (0.5 ML). It is thus concluded that adsorption sites on the Ti(0001) surface have been filled by "resurfacing" H atoms supplied from the Ti bulk. This is plausible as in the high-temperature range (900–400 K) of the rapid surface H emergence the energetically favorable and vacant surface chemisorption sites are accessible for a large number of H atoms diffusing in the bulk. At the bulk H concentration of ~500 ppm, an equivalent of 1 ML H is contained in ~2000 layers of Ti atoms, i.e., in a volume of ~470 nm depth in the [0001] direction (lattice constant $c = 4.68$ Å), so that within 1 s ~ 42 ML H can reach the surface at 900 K (diffusion length $L_D = 20$ μm/s). At 400 K, this figure totals only 0.6 ML ($L_D = 277$ nm/s), which explains the saturation of the surface H buildup upon further cooling as the H mobility in the Ti bulk freezes in before all surface sites are filled. A similar emergence of bulk-dissolved H atoms on the (110) and (111) surfaces of Pd has also been reported.[27,28]

To characterize the thermal activation behavior of surface and near-surface absorbed H atoms on Ti(0001) in comparison to Pd(100), the Ti(0001) surface was saturated with a large dose of H_2 (12000 L) at 120 K. The corresponding NRA γ-yield curve (Fig. 5) indicates (by the asymmetric broadening on the high energy side of the surface resonance peak) that these exposure conditions cause simultaneous H absorption into shallow depths below the surface (1–2 nm), and that the total H uptake exceeds 1 ML (1.3 ± 0.1 ML). As the absorbed H near the surface is not clearly resolved from the Doppler-broadened surface H signal, we can neither specify the surface saturation coverage nor the amount of absorbed H atoms from these data with certainty. A H_2 thermal desorption spectrum of this H-saturated Ti(0001) surface is shown in Fig. 6. Only spurious H_2 desorption signals are recognizable in the entire temperature range between 120 and 650 K. Yet above a threshold of ~650 K massive H_2

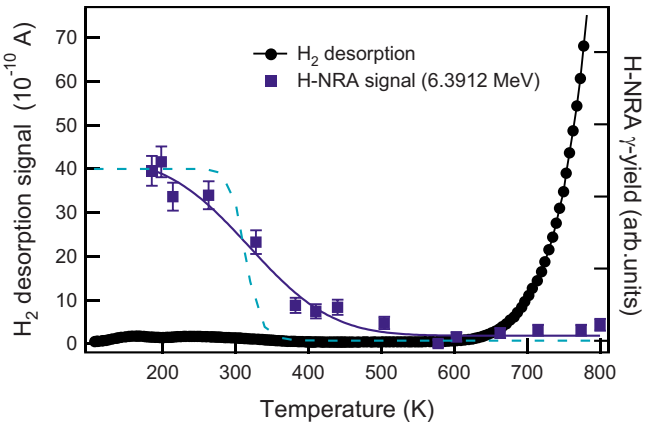

FIG. 6. (Color online) H_2 thermal-desorption spectrum of a H-saturated Ti(0001) single-crystal surface (12000 L H_2 at 100 K) compared to the temperature dependence of the NRA signal of surface hydrogen (θ_s=0.5 ML at 180 K). The dashed line indicates the calculated H surface occupation in thermal equilibrium with the Ti bulk for ε_s=−1.05 eV.

evolution was recorded that rose exponentially with the crystal temperature. This is shown only partially in Fig. 6, as the axes are scaled to the same range as the TDS trace of Pd(100) for comparison (Fig. 2). At the maximum TDS ramp temperature of 970 K the H_2 desorption signal from Ti(0001) exceeded the desorption peak intensity of 1 ML H/Pd(100) at 330 K (Fig. 2) by 2 orders of magnitude. An Arrhenius plot of the H_2 desorption intensity in the 700–970 K range (Fig. 7) assumes a straight line with excellent statistics and high reproducibility over numerous TDS runs, the slope (E_a =0.46±0.02 eV/atom) being in close agreement with the heat of H solution in the Ti α-phase. Even as the Ti(0001) sample cooled back to 700 K after sudden heating termination at 970 K, the H_2 desorption signal exhibited exactly the

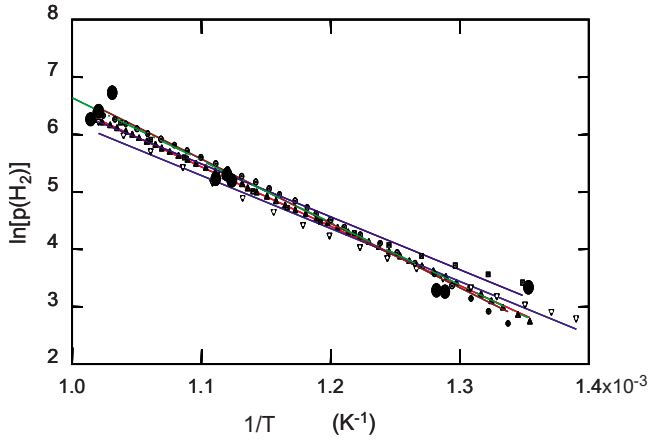

FIG. 7. (Color online) Arrhenius plot of the H_2 desorption rate from the Ti(0001) bulk at temperatures >700 K for several TDS runs, including the T dependence of p(H_2) during cooling from the maximum (T_{max}) of the heating ramp to 700 K. To demonstrate the reproducibility without increasing the data point density beyond readability, H_2 pressures measured at T_{max} of several heating runs (large points) are also shown. The average of the fitted slopes corresponds to an activation energy of E_a=0.46±0.02 eV per H atom.

same temperature dependence as during the TDS heating ramp. This indicates that the intense H_2 release above the ~650 K threshold originates from the Ti bulk, in an attempt of the system to establish thermal equilibrium between the bulk-dissolved H and the surrounding gas phase H_2(p≤1 ×10^{-6} Pa).

Complementing the TDS spectrum in Fig. 6 the temperature-dependent signal of surface H on Ti(0001) between 180 and 800 K is shown. These NRA data were measured by incrementally heating the sample after preparing an initial coverage of $\theta_H \approx 0.5$ ML resurfaced H as described above, using the same ^{15}N ion energy as in Fig. 4. Starting at 180 K, the H coverage decreased in a broad decay between 200 and 500 K until only the continuous bulk H concentration remained detectable above 600 K. In notable contrast to the behavior of H/Pd(100) no simultaneous H_2 desorption was detected in the TDS spectrum, not even for the surface in fully H_2-saturated condition that included absorbed H closely below the surface (Fig. 5). We therefore conclude that at any H coverage up to saturation thermal activation causes the chemisorbed H atoms to penetrate from the Ti(0001) surface into the Ti subsurface, from where they escape out of the depth detection range of the NRA measurement by diffusion into the deeper bulk. Obviously, a facile exchange of H atoms between the Ti(0001) surface and the Ti bulk is taking place between ~250 and 650 K without noteworthy desorption loss of H_2.

IV. DISCUSSION

A. Competition of desorption and bulk absorption

1. Kinetics

The presented NRA/TDS data indicate clearly that thermal activation of chemisorbed H atoms causes desorption of H_2 from Pd(100), whereas bulk absorption of these H atoms results in case of Ti(0001). In order to determine the factors responsible for this opposite behavior of two commonly hydride-forming metals, we first discuss the kinetics of the hydrogen transition between the gas phase and the metal bulk. For this purpose it has become customary in the literature to illustrate the energy barriers of the elemental reaction steps in simplified, one-dimensional "reaction coordinate" diagrams. We partially followed this tradition in Fig. 8, which schematically visualizes the energy barriers of H_2 desorption (E_{des}), surface penetration of H atoms into first-layer subsurface sites (E_{pen}), resurfacing (E_{res}) and bulk absorption (E_{abs}) of H atoms from subsurface sites, as well as the activation energy of H diffusion in the bulk (E_{diff}). The diagram also indicates the energy levels of H atoms on the surface (ε_s), in the bulk (ε_b=ΔH_s, heat of solution) and in subsurface sites (ε_{ss}), with reference to the metal and H_2 at infinite separation (dashed line). The subsurface sites, in which the H energy may differ from that of H on the surface as well as from that of H in the bulk,[29] are included for completeness only, since it is sometimes stated that they may strongly influence the hydrogen absorption kinetics.[30] We will briefly comment on this in Sec. IV C. Most importantly, however, we point out two significant differences of our representation

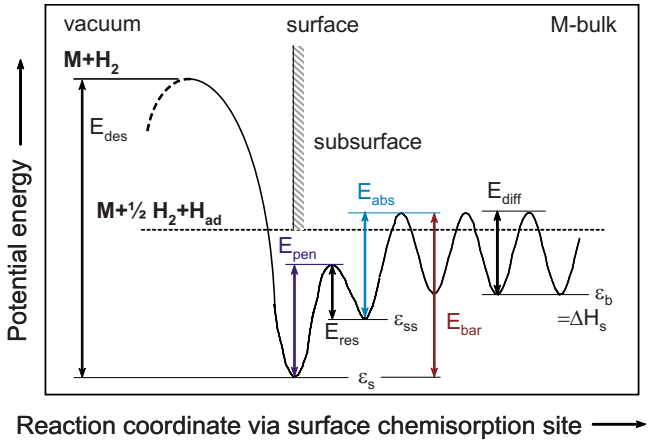

FIG. 8. (Color online) Schematic one-dimensional energy diagram visualizing the kinetic barriers encountered by H atoms chemisorbed on a metal surface (m) for the competing reactions of recombinative desorption and bulk absorption.

from similar potential-energy diagrams frequently found in the literature, e.g., Ref. 14.

First, we explicitly define the reaction coordinate for the hydrogen absorption such that the minimum of the surface chemisorption well represents the majority adsorption site on a well-ordered single-crystal surface. This reflects our objective (and experimental situation) to clarify whether the regular terrace chemisorption sites on H-saturated surfaces (as opposed to defects) represent possible starting points for H absorption into the bulk.

Second, our reaction coordinate connects the surface chemisorption site with gaseous H_2 in the molecular state, because atomic H desorption was never observed and H_2 desorption requires recombination of two chemisorbed H atoms. Consequently, the relevant kinetic-energy barrier E_{des} determining the H coverage (θ_s) reduction rate due to molecular H_2 desorption corresponds to $E_{\mathrm{des}}=-2\times\varepsilon_s$, where ε_s is the adsorption energy per H atom. It is important to note that in many cases similar diagrams in the literature[14] draw a "reaction coordinate" for a single H atom that links the bottom of the chemisorption well with the energy of $1/2H_2$ in the gas phase at infinite distance from the metal (M) surface without indicating the second H atom on the surface (H_{ad}) that takes part in the recombination to H_2, thus apparently $E_{\mathrm{des}}=-\varepsilon_s$. It should be emphasized that such representations are first and foremost convenient to illustrate the enthalpy differences of H atoms on the surface (ε_s) and in the bulk metal (ε_b) in thermal equilibrium with the gas phase, or the total energy of the H_2+M system as a H_2 molecule approaches and dissociates on the surface. In this form, however, they give a rather misleading impression of the kinetic barrier height encountered in the diatomic desorption event compared to those of the monoatomic transitions of H atoms between sites on the surface, the subsurface, and in the bulk with their individual activation energies E_k (Fig. 8). Recognizing the fact that both monoatomic and diatomic processes occur at the surface, we have therefore purposely dropped the intention to depict the entire transition of gas phase H_2 to atomic H in the metal bulk on a continuous one-dimensional reaction coordinate and omitted the H_2 dissociation and equilibrium energetics (inclusion of which would require a multidimensional potential-energy surface). Consequently, Fig. 8 focuses strictly on illustrating only the kinetic-energy barriers of reactions involving surface H atoms as they are directly observable as activation energies in the thermal activation experiment. The figure is thus the direct graphical translation of the kinetic reaction-rate equations describing associative desorption and bulk-absorption of surface H. Note that the left part involves two surface H atoms, the right part only one. It is neither meant to claim that H atoms attain an energy level of $+|\varepsilon_s|$ after desorption into the gas phase at thermal equilibrium, nor that a single H atom would have to bear the entire desorption activation energy E_{des}.

TABLE I. Energies of H surface adsorption (ε_s), bulk dissolution ($\Delta H_s=\varepsilon_b$) (Refs. 12 and 13), and activation energies (E_{diff}) and exponential prefactors of the H bulk diffusion coefficient (D_0) (Ref. 31) for H on/in Pd, Ti, and Ni.

	ε_s (eV)	$\Delta H_s=\varepsilon_b$ (eV)	E_{diff} (eV)	D_0 ($\mathrm{cm^2\ s^{-1}}$)
Pd	−0.53 [a]	−0.1	0.23	2.9×10^{-3}
Ti	−(0.95−1.05) [b]	−0.47	0.53	3.64×10^{-3}
	−0.92 [c]	-0.46 ± 0.02 [c]		
Ni	−0.5 [d]	+0.17	0.41	4.8×10^{-3}

[a]Pd(100), Reference 2.
[b]References 8–11.
[c]This work.
[d]Reference 32.

The key implication regarding the kinetic competition between the desorption and bulk-absorption rates of chemisorbed H atoms is apparent from the comparison of the activation energy for the recombinative desorption, $E_{\mathrm{des}}=-2\varepsilon_s$, relative to the minimum effective energy barrier, E_{bar}, that a chemisorbed H atom has to overcome in order to be absorbed into the bulk. Figure 8 indicates that E_{bar} relates to the energy difference of H on the surface versus H in the bulk and to the activation energy for bulk diffusion, i.e., $E_{\mathrm{bar}}=-(\varepsilon_s-\varepsilon_b)+E_{\mathrm{diff}}$. We hence expect predominant absorption (desorption) to occur if $E_{\mathrm{des}}>(<)E_{\mathrm{bar}}$, or $-\varepsilon_s>(<)E_{\mathrm{diff}}+\varepsilon_b$. Where necessary, this kinetic criterion is easily extended to systems in which H_2 dissociation is activated by an energy barrier E_{diss}: H absorption (desorption) results for $E_{\mathrm{des}}=E_{\mathrm{diss}}-2\varepsilon_s>(<)-(\varepsilon_s-\varepsilon_b)+E_{\mathrm{diff}}$. Table I compares the quantities ε_s, ε_b, and E_{diff} for Pd, Ti, and Ni, which reveals that H absorption is kinetically favorable for both Pd and Ti ($E_{\mathrm{des}}>E_{\mathrm{bar}}$), mainly as a consequence of their large surface adsorption energies and exothermic H absorption properties. On Ni the H adsorption energy ε_s is similar as on Pd, but H absorption is endothermic ($\varepsilon_b>0$). Here, the kinetic criterion ($E_{\mathrm{des}}<E_{\mathrm{bar}}$) reasonably accounts for H_2 desorption from Ni surfaces, as experimentally observed.[32] The expectation of H absorption by Ti(0001) likewise agrees well with our experiment.

In case of Pd(100), however, the predicted H absorption is in obvious conflict with the observed H_2 desorption. We note that the $E_{\mathrm{des}}>-(\varepsilon_s-\varepsilon_b)+E_{\mathrm{diff}}$ relation holds even if a pos-

sible influence of the H coverage on ε_s is taken into account, and that the model's predictions do not change if also the kinetic prefactors entering the rates of desorption and absorption are considered. Since the adsorption energy for H/Pd(100) is only weakly coverage dependent[2] and ε_s for H/Ti(0001) was calculated to–(0.95–1.05) eV/atom at full coverage by several groups,[8–11] it appears justified to consider variations of ε_s small. Further support to assume ε_s coverage independent is given by the fact that neither of the surfaces shows signs of geometrical reconstructions upon hydrogen adsorption. The exponential prefactor for monoatomic H absorption, approximately 10^{13} s^{-1}, is of the time scale of atomic vibrations, hence certainly not smaller than the frequency factor of the diatomic H_2 recombination. Including these details thus only furthers the expectation that the recombinative H_2 desorption rate is slow compared to H absorption for both Ti and Pd. To reconcile with the observed H_2 desorption from Pd(100), one may consider an additional kinetic impediment for H absorption, e.g., a steep surface penetration (E_{pen}) barrier that may exceed even E_{des}, so that H_2 desorption might become the faster reaction in spite of $E_{des} > E_{bar}$. However, our NRA/TDS observation that the absorbed near-surface hydride phase decomposes independently from and desorbs at much lower temperature (185 K) than the layer of surface H atoms (T_{des}=330 K, Fig. 2) puts serious doubt on the existence of a profound penetration barrier on Pd(100), since due to microscopic reversibility $E_{pen} > E_{des}$ should also prevent H in subsurface sites from desorption and instead cause its absorption into the bulk upon warming. On the contrary, the desorption of the absorbed H at 185 K proves that a separate reaction coordinate must exist that connects gaseous H_2 directly with the H atoms in the subsurface but does not involve the H chemisorption well on Pd(100). For this reason such a pathway is not indicated in Fig. 8, which by definition considers only H transitions via regular surface chemisorption sites.

Estimates of the H penetration barrier heights from Pd(111) fcc hollow sites into the octahedral first-layer subsurface interstitials based on density-functional theory predict E_{pen}=0.85–0.4 eV,[33] and E_{pen}=0.3–0 eV,[34] where the smaller values are obtained if the concerted motion of the Pd atoms upon H absorption (relaxation) is taken into account. This suggests that $E_{pen} < E_{bar} < E_{des}$ on Pd(111), Pd(110) and Pd(210), i.e., no *kinetic* hindrances for bulk absorption of surface H are expected to prevail at all on these more "open" surfaces, and the resurfacing of bulk-absorbed H on Pd(110), and Pd(111) reported earlier[27,28] confirms that no profound penetration barrier exists on these surfaces. Nonetheless, experimentally H_2 desorbs from all Pd surfaces [including (100)] at similar temperatures around 300–350 K.[2–5] Thus, considerations of kinetic barrier heights alone are obviously insufficient to correctly describe the response of surface H atoms to thermal activation, and the principal behavior seems to be rather insensitive to the particular surface crystallography. Apparently other important factors exist that decisively affect the competition between H_2 desorption and H bulk absorption.

2. H solubility and diffusion

We argue in the following that an additional thermodynamic condition needs to be fulfilled simultaneously for H absorption to occur. The critical issue is whether accommodating the layer of surface H atoms into the bulk of the metal is energetically favorable around the temperature at which the H atoms detach from their bonds to the surface. We suggest that the fate of the surface H can be predicted by estimating whether the solubility of the metal allows incorporating the surface H atoms into a slab of bulk metal that extends from the surface into a depth approximately determined by the diffusion length of the H atoms at the "detachment" temperature T_{det}, at which the H bonds to the surface break. For the easily observable H_2 desorption, T_{det} is straightforwardly identified with the H_2 desorption peak temperature of surface H, whereas in cases of H absorption T_{det} can be obtained from an analysis of the temperature-dependent H coverage.

We estimate the surface hydrogen coverage that can be dissolved into the bulk by in-diffusion. At any temperature the dissolvable amount of surface H can roughly be approximated by the product of the equilibrium H solubility and the H diffusion length $L_D=(D\Delta t)^{1/2}$ in the bulk as calculated from the H diffusion coefficient $D(T)=D_0\times\exp(-E_{diff}/k_BT)$ (Table I), which is conveniently expressed in monolayers (ML) after division by the atomic layer distance between neighboring H interstitial sites, i.e., by one half of the lattice constant d_L in case of face-centered-cubic (Pd) or hexagonal (Ti) metals. The H solubility (H molar fraction) x_H in thermal equilibrium with a surrounding gas phase at a pressure $p(H_2)$ is given by[13]

$$x_H = \left(\frac{p_{H_2}}{p_0}\right)^{1/2} \exp\left(\frac{\Delta S_s}{k_B}\right)\exp\left(-\frac{\Delta H_s}{k_BT}\right) \quad (1)$$

from which we obtain the following general expression for the temperature dependence of the bulk-dissolvable H coverage θ_{solv}:

$$\theta_{solv} = \frac{2}{d_L}\left(D_0\Delta t\frac{p_{H_2}}{p_0}\right)^{1/2} \times\exp\left(-\frac{\Delta H_s - T\Delta S_s + \frac{1}{2}E_{diff}}{k_BT}\right) \text{ (in ML)}. \quad (2)$$

ΔS_s and ΔH_s are the entropy and enthalpy changes upon H_2 solution in the metal α-phase, and the standard pressure is $p_0=10^5$ Pa. For both Pd and Ti, $\Delta S=-7k_B$ (Ref. 13) (k_B: Boltzmann constant), ΔH_s, D_0 and E_{diff} values are given in Table I. Parameters of the TDS experiment enter as the H_2 background pressure ($p(H_2)\sim 1\times10^{-7}$ Pa) and the time scale of the diffusion process Δt, which is approximated by the width of the thermal desorption peak and the given heating rate (in our case: $\Delta t\sim 100$ s). The dissolvable amount of surface hydrogen is shown in Fig. 9 for the above conditions and the respective lattice constants d_L, i.e., (a=3.90 Å) for Pd(100) and (c=4.86 Å) for Ti(0001). It is seen that 1 ML surface H on Ti(0001) can easily be absorbed between 180 and 600 K, in agreement with our experiment (Fig. 6). The H solubility in thermal equilibrium [Eq. (1)] is additionally limited by the maximum stoichiometry of TiH_2(x_H=2), which is reached at ~260 K for $p(H_2)=1\times10^{-7}$ Pa. Below 260 K the H dissolution is therefore restricted mainly by the H mo-

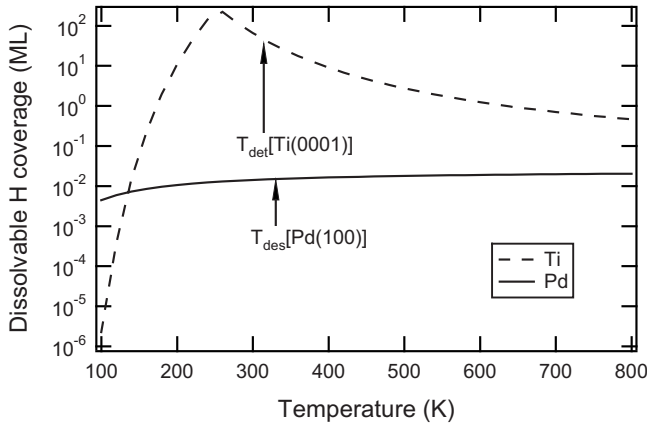

FIG. 9. Amount of bulk-absorbable surface hydrogen (in ML) by Pd and Ti at $p(H_2)=1\times10^{-7}$ for a diffusion time of $\Delta t=100$ s in Eq. (2). The respective desorption and "detachment" temperatures of surface H from Pd(100) and Ti(0001) are indicated.

bility, which becomes severely suppressed as the H diffusion length drops below one atomic layer distance at 180 K. Consistently, we observe that at 120 K the H uptake by our H_2-exposed Ti(0001) sample saturates near the surface (Fig. 5). In contrast to Ti, the surface H quantity absorbable by Pd is much smaller (1%–2% ML between 200 and 800 K) and only weakly temperature dependent, because for Pd coincidentally ΔH_s and $1/2E_{\mathrm{diff}}$ nearly cancel in the exponential term of Eq. (2). $1/2E_{\mathrm{diff}}$ even slightly dominates, causing an overall increase in the absorbable H coverage with temperature although H absorption in Pd is exothermic. Regarding our thermal activation experiment, Fig. 9 indicates that the initial coverage of 1 ML H on Pd(100) cannot be accommodated into the Pd bulk on the time scale of the TDS heating ramp, which explains the observed H_2 desorption from the Pd(100) surface. Therefore, although H absorption by Pd(100) would be kinetically "allowed," this process is "overruled" by the thermodynamic restriction to dissolve the surface H into the bulk during the thermal activation experiment. Under the latter conditions, the opposite behavior of surface H atoms on Pd(100) and Ti(0001) is thus readily understood. Naturally, thermodynamics do not principally exclude surface-H absorption by Pd; Eq. (2) and Fig. 9 indicate that this may only require higher H_2 pressures and longer observation times.

B. H/Ti(0001): adsorption energy

Despite the fundamental importance of the H/Ti(0001) system, e.g., for the titanium sublimation pump, no experimental data have been published that would reliably reveal the depth of the H chemisorption well on Ti(0001), and the information available today stems mainly from theory.[8–11] Presumably the facile exchange of H atoms between the surface and the bulk of Ti described here has so far precluded a clear experimental distinction of the heat of H adsorption and bulk dissolution, because TDS cannot deliver the heat of adsorption in the conventional manner due to the lack of a distinct desorption peak (Fig. 6). Our NRA observation that dissolved H atoms "resurface" from the Ti bulk when the flash-heated sample cools in vacuum (Fig. 4) is therefore by no means trivial, but should rather be regarded as a rare experimental indication that H atoms in surface adsorption sites *are* in fact energetically more stable than in the Ti bulk. A noteworthy consequence of this circumstance is the impossibility to prepare a clean and well-ordered Ti(0001) surface entirely free of H as long as there are still trace amounts of H dissolved in the bulk. In addition to the high surface reactivity toward H_2, this poses a serious problem for the accurate determination of the surface relaxation of Ti(0001), which reportedly is quite sensitive to the presence of adsorbed H.[11,35,36]

The depth of the surface chemisorption potential for H on Ti(0001) can be estimated from our NRA measurement of the temperature-dependent H coverage (Fig. 6). The first possible interpretation of these data is one of a kinetic reaction transient (surface-to-bulk transition of H atoms), for which effective first-order kinetics should apply. By fitting the data to an inverse cumulative distribution (solid line in Fig. 6), the temperature of maximum H coverage reduction rate can be determined as the inflection point of the H coverage decay, i.e., $T_m=318\pm22$ K. From this and the well-known Redhead approximation[37] for first-order desorption with a frequency factor of 10^{13} s^{-1} and a heating rate of 1 K/s an activation energy $E_a=0.88\pm0.07$ eV is derived. With reference to Fig. 8, this activation energy is identified as the surface-to-bulk-absorption barrier E_{bar}. With $E_{\mathrm{bar}}=-(\varepsilon_s-\varepsilon_b)+E_{\mathrm{diff}}$, we obtain $\varepsilon_s=-0.82\pm0.07$ eV. An earlier experimental report of −0.75 eV/atom for H_2 adsorption on Ti film[6] is somewhat smaller, which might be due to overlap with beginning bulk-absorption that is difficult to rule out in a calorimetric measurement. The considerable width of the H coverage decay in Fig. 6, however, indicates that this transient is likely broadened by H in- (and back-) diffusion, thus the applicability of the kinetic Redhead formalism may be questioned. The second possible interpretation of the temperature-dependent H coverage is conceivable in that it may reflect thermal equilibrium between H on the Ti(0001) surface and H in the Ti bulk. In terms of statistical thermodynamics their relative occupation is described by a two energy-level system $(\varepsilon_s,\varepsilon_b)$, where the degeneracy of the higher state (ε_b) increases with temperature as the number of available bulk sites grows exponentially with the diffusion length from the surface, similar as in Eq. (2). By modeling this system with ε_s as a parameter, we find reasonable agreement with the experimental inflection temperature T_m for $\varepsilon_s=-1.05\pm0.1$ eV, as indicated by the dashed line in Fig. 6. Again, the width of the experimental coverage decay is obviously much larger than this calculated temperature dependence, suggesting that on the time scale of our measurement the establishment of the surface/bulk thermal equilibrium was delayed by H in- (and back-) diffusion. Apparently, in the present case the bidirectional H diffusion between the surface and the Ti bulk does not allow for an accurate description of our data in neither a purely kinetic nor a purely thermodynamic model, although both yield comparable estimations of ε_s in fair agreement with theoretical results ($\varepsilon_s=-0.95-1.05$ eV).[8–11]

For an ε_s evaluation based on fewer assumptions we recall the temperature threshold for H_2 evolution from the Ti bulk at 650 K. By rearranging Eq. (1) it is realized that the equilibrium H_2 pressure over our Ti(0001) specimen with 500 ppm bulk H exceeds 1×10^{-7} Pa already at 415 K, i.e., the H_2 release should evolve at a considerably lower temperature than in Fig. 6. Hence, apparently the attainment of thermal equilibrium between the Ti bulk and gas phase H_2 is kinetically hindered below 650 K. Using this threshold in a Redhead approximation to obtain the height of the H-retaining barrier yields 1.84 eV, i.e., 0.92 eV/H atom. Figure 8 suggests identifying this 0.92 eV barrier with $-\varepsilon_s$. Our inherent assumption inferred from the high surface reactivity[8] that there is no activation barrier for the dissociative adsorption of H_2 on Ti(0001) is supported by recent first-principles calculations.[38]

C. H transitions between the surface and the bulk

Finally, the mechanism of the reversible transition of H atoms between the Ti bulk and the Ti(0001) surface deserves some further attention. Combined with the H resurfacing from the bulk after annealing (Fig. 4), the above H-retaining effect presented by the deep surface chemisorption well implies that H atoms do not directly transit from the Ti bulk into the gas phase (which should occur with an activation threshold of $-\Delta H_s=0.46$ eV, Fig. 8), but first populate the chemisorption sites on the (0001) surface before they recombine to H_2 and desorb. This remarkably contrasts the desorption pathway of subsurface-absorbed H from Pd(100). Here, the chemisorption sites are bypassed at 185 K, which points toward the existence of a separate reaction coordinate linking the subsurface sites directly to the gas phase.[14,39] This feature may not be peculiar to Pd(100) alone, as bypassing of the chemisorption sites was also observed during low-temperature (80 K) H_2 subsurface absorption by and desorption from Pd(111).[40] On the other hand, H transitions into the subsurface starting from regular Pd(111) surface sites are only moderately activated and occur above 250 K.[41] Yet, subsurface site population does not necessarily imply the completed bulk absorption of the H atoms, because the Pd(111) subsurface H state is energetically very close to the surface chemisorption site ($\varepsilon_s\approx\varepsilon_{ss}$) (Ref. 42) so that a major part of the energy barrier for the transition into the bulk (E_{bar}, cf. Fig. 8) still remains to be surmounted. Whether a complete "drainage" of surface H atoms into the bulk similar as on Ti(0001) would be observable on Pd(111) below the desorption temperature (possibly on a longer timescale, cf. Fig. 9) therefore remains an open question that may deserve further investigation. A rapid equilibration between the surface-adsorbed and near-surface absorbed H as observed in molecular-beam experiments on Pd(111) by Engel *et al.*[28] was reported only above room temperature.

In this context it is worthwhile to comment on the role of the subsurface state on the H absorption kinetics.[30] By modeling the respective rates of bulk absorption of surface H for the experimentally determined parameters of ε_s, ε_b, and E_{diff}, and including a small number of subsurface states (up to five) at a variable energy level ε_{ss} between ε_s and ε_b (cf. Fig. 8), we observed that the subsurface states impose only tiny delays of the H arrival from the surface in the bulk sites beneath the subsurface layers. These delays are many orders of magnitude too small as to be noticed on the time and temperature scale of our heating experiment ($\sim$1 K/s, $T>250$ K). Our simulations show that surface and subsurface occupations rapidly equilibrate in a stationary state within a few diffusion jumps, after which ε_{ss} cancels out in the total expression for the H transfer rate from the surface into the bulk. The decisive barrier for the surface-to-bulk diffusion then remains E_{bar}, which does not depend on ε_{ss} (for $\varepsilon_s<\varepsilon_{ss}<\varepsilon_b$) as seen in Fig. 8. Hence, H absorption in subsurface states becomes a dominating effect only under experimental conditions, where the total amount of absorbed H is small and where it is confined to a region very close to the surface, e.g., at low H_2 exposure temperatures, when the diffusion into the deeper bulk is thermally restricted. On the other hand, for the overall surface-to-bulk transfer occurring at higher temperatures, where bulk diffusion is enabled so that absorption of hydrogen quantities exceeding a few ML becomes possible, the role of the subsurface states should not be overestimated.

At present, it is concluded that H exchange between the surface and the Ti bulk proceeds efficiently via regular surface chemisorption sites on Ti(0001). In contrast, it appears that on Pd(100) minority sites[14] (probably defects of smaller $|\varepsilon_s|$) are far more effective for H transitions into the bulk (under favorable thermodynamic conditions for H absorption), leaving chemisorbed H a bypassed spectator. From an engineering standpoint, our kinetic considerations further suggest that reducing the surface adsorption energy (ε_s) of metals is a promising strategy to improve the speed of H absorption/desorption, i.e., by tailoring E_{bar}. The feasibility of this approach has already been demonstrated, e.g., for Pd-coated niobium.[43] The same idea is also reflected in very recent indications that the energetic destabilization of surface H by coadsorbed carbon may enhance the rate of the surface-to-bulk-transition of adsorbed H atoms into the volume of oxide-supported Pd nanocrystals, which has important implications for the industrial catalysis of olefin hydrogenations.[44]

V. CONCLUSION

Based on the observation of an entirely opposite behavior of H atoms adsorbed on Pd(100) and Ti(0001) surfaces upon thermal activation in vacuum we have elucidated the competition between recombinative H_2 desorption and bulk absorption of H on metal surfaces. Consequently separate kinetic and thermodynamic considerations lead to a set of two criteria that allow predicting whether desorption or bulk absorption occurs: In addition to the barrier height for the H surface-to-bulk transition relative to that of H_2 desorption the H solubility in the metal bulk is a key parameter. Evaluating the two conditions is straightforward and only requires knowledge of three quantities: ε_s, ε_b, and E_{diff}. For strongly exothermic H absorbers such as Ti, the H surface adsorption energy ε_s as well as the characteristic "detachment" temperature, at which H penetrates from the surface into the bulk, are likely to be unknown due to the limitations of conventional

thermal-desorption spectroscopy. NRA can provide this missing-link information by delivering the temperature-dependent H coverage in addition to the thermal stability and depth distribution of absorbed H species on a nanometer scale. The combined techniques can thus reveal fundamental insight into the transition mechanism of H atoms between the gas phase, the surface, and the bulk of metals. This detailed understanding of the H absorption/release process is considered vital for the development of metal hydride-based hydrogen storage technology.

ACKNOWLEDGMENTS

The provision of the Ti(0001) single crystal by Y. Mizuno and fruitful discussions with Y. Murata and Y. Fukai are greatly appreciated. The authors are grateful to the Ministry of Education, Science, Sports and Culture of Japan for financial support through a Grant-in-Aid for Basic Scientific Research. Assistance in the MALT accelerator operation by H. Matsuzaki and C. Nakano is gratefully acknowledged.

*Corresponding author. FAX: +81-3-5452-6159; wilde@iis.u-tokyo.ac.jp (M. Wilde)

[1] K. Christmann, Surf. Sci. Rep. **9**, 1 (1988).
[2] R. J. Behm, K. Christmann, and G. Ertl, Surf. Sci. **99**, 320 (1980).
[3] G. E. Gdowski, T. E. Felter, and R. H. Stulen, Surf. Sci. **181**, L147 (1987).
[4] H. Conrad, G. Ertl, and E. E. Latta, Surf. Sci. **41**, 435 (1974).
[5] U. Muschiol, P. K. Schmidt, and K. Christmann, Surf. Sci. **395**, 182 (1998).
[6] G. F. Wedler and H. Strothenk, Z. Phys. Chem. **48**, 86 (1966).
[7] P. J. Feibelman and D. R. Hamann, Phys. Rev. B **21**, 1385 (1980).
[8] P. J. Feibelman, D. R. Hamann, and F. J. Himpsel, Phys. Rev. B **22**, 1734 (1980).
[9] P. Cremaschi and J. L. Whitten, Phys. Rev. Lett. **46**, 1242 (1981).
[10] P. Cremaschi and J. L. Whitten, Surf. Sci. **112**, 343 (1981).
[11] M. N. Huda and L. Kleinman, Phys. Rev. B **71**, 241406(R) (2005).
[12] W. M. Mueller, J. P. Blacklegde, and G. G. Libowitz, *Metal Hydrides* (Academic, New York, 1968).
[13] Y. Fukai, *The Metal Hydrogen System* (Springer, Berlin, 2005).
[14] H. Okuyama, W. Siga, N. Takagi, M. Nishijima, and T. Aruga, Surf. Sci. **401**, 344 (1998).
[15] M. Wilde, M. Matsumoto, K. Fukutani, and T. Aruga, Surf. Sci. **482-485**, 346 (2001).
[16] J. W. Davenport, G. J. Dienes, and R. A. Johnson, Phys. Rev. B **25**, 2165 (1982).
[17] W. A. Lanford, Nucl. Instrum. Methods Phys. Res. B **66**, 65 (1992).
[18] W. A. Lanford, *Handbook of Modern Ion Beam Materials Analysis*, edited by J. llR. Tesmer and M. Nastasi (Materials Research Society, Pittsburgh, 1995), p. 193.
[19] M. Zinke-Allmang, S. Kalbitzer, and M. Weiser, Z. Phys. A **320**, 697 (1985).
[20] F. Fujimoto, Nucl. Instrum. Methods Phys. Res. B **45**, 49 (1990).
[21] N. Rud, J. Boettinger, and P. S. Jensen, Nucl. Instrum. Methods **151**, 247 (1978).
[22] B. Maurel and G. Amsel, Nucl. Instrum. Methods Phys. Res. **218**, 159 (1983).
[23] K. Fukutani, A. Itoh, M. Wilde, and M. Matsumoto, Phys. Rev. Lett. **88**, 116101 (2002).
[24] J. F. Ziegler, *Handbook of Stopping Cross-Sections for Energetic Ions in All Elements* (Pergamon, New York, 1980).
[25] M. Wilde and K. Fukutani, Nucl. Instrum. Methods Phys. Res. B **232**, 280 (2005).
[26] M. Wilde, K. Fukutani, S. Koh, K. Sawano, and Y. Shiraki, J. Appl. Phys. **98**, 023503 (2005).
[27] M. G. Cattania, V. Penka, R. J. Behm, K. Christmann, and G. Ertl, Surf. Sci. **126**, 382 (1983).
[28] T. Engel and H. Kuipers, Surf. Sci. **90**, 162 (1979).
[29] S. Wilke, D. Hennig, R. Löber, M. Methfessel, and M. Scheffler, Surf. Sci. **307-309**, 76 (1994).
[30] J. Rogan, M. Lagos, and I. K. Schuller, Surf. Sci. **318**, L1165 (1994), and references therein.
[31] H. Wipf, in *Hydrogen in Metals III*, Topics in Applied Physics Vol. 73 (Springer, Berlin, 1997).
[32] K. Christmann, O. Schober, G. Ertl, and M. Neumann, J. Chem. Phys. **60**, 4528 (1974).
[33] K. Nobuhara, H. Kasai, H. Nakanishi, and A. Okiji, J. Appl. Phys. **92**, 5704 (2002).
[34] O. M. Løvvik and R. A. Olsen, Phys. Rev. B **58**, 10890 (1998).
[35] P. J. Feibelman, Phys. Rev. B **53**, 13740 (1996).
[36] G. Teeter and J. L. Erskine, Phys. Rev. B **61**, 13929 (2000).
[37] P. A. Redhead, Vacuum **12**, 203 (1962).
[38] K. Nobuhara, H. Kasai, W. A. Diño, and H. Nakanishi, Surf. Sci. **566-568**, 703 (2004).
[39] G. Comsa, R. David, and B.-J. Schumacher, Surf. Sci. **95**, L210 (1980).
[40] G. E. Gdowski, R. H. Stulen, and T. E. Felter, J. Vac. Sci. Technol. A **5**, 1103 (1987).
[41] W. Eberhardt, S. G. Louie, and E. W. Plummer, Phys. Rev. B **28**, 465 (1983).
[42] M. S. Daw and S. M. Foiles, Phys. Rev. B **35**, 2128 (1987).
[43] M. A. Pick, J. W. Davenport, M. Strongin, and G. J. Dienes, Phys. Rev. Lett. **43**, 286 (1979).
[44] M. Wilde, K. Fukutani, W. Ludwig, B. Brandt, J.-H. Fischer, S. Schauermann, and H.-J. Freund, Angew. Chem., Int. Ed. (to be published).